Mechanisms of β-Adrenergic Modulation of I_{Ks} in the Guinea-Pig Ventricle: Insights from Experimental and Model-Based Analysis

Stefano Severi,[†] Cristiana Corsi,[†] Marcella Rocchetti,[‡] and Antonio Zaza[‡*]
[†]Biomedical Engineering Laboratory–D.E.I.S., University of Bologna, Cesena, Italy; and [‡]Dipartimento di Biotecnologie e Bioscienze, Università di Milano-Bicocca, Milano, Italy

ABSTRACT Detailed understanding of I_{Ks} gating complexity may provide clues regarding the mechanisms of repolarization instability and the resulting arrhythmias. We developed and tested a kinetic model to interpret physiologically relevant I_{Ks} properties, including pause-dependence and modulation by β-adrenergic receptors (β-AR). I_{Ks} gating was evaluated in guinea-pig ventricular myocytes at 36°C in control and during β-AR stimulation (0.1 μmol/L isoprenaline (ISO)). We tested voltage dependence of steady-state conductance (Gss), voltage dependence of activation and deactivation time constants (τ_{act}, τ_{deact}), and pause-dependence of τ_{act} during repetitive activations (τ_{react}). The I_{Ks} model was developed from the Silva and Rudy formulation. Parameters were optimized on control and ISO experimental data, respectively. ISO strongly increased Gss and its voltage dependence, changed the voltage dependence of τ_{act} and τ_{deact}, and modified the pause-dependence of τ_{react}. A single set of model parameters reproduced all experimental data in control. Modification of only three transition rates led to a second set of parameters suitable to fit all ISO data. Channel unitary conductance and density were unchanged in the model, thus implying increased open probability as the mechanism of ISO-induced Gss enhancement. The new I_{Ks} model was applied to analyze ISO effect on repolarization rate-dependence. I_{Ks} kinetics and its β-AR modulation were entirely reproduced by a single Markov chain of transitions (for each channel monomer). Model-based analysis suggests that complete opening of I_{Ks} channels within a physiological range of potentials requires concomitant β-AR stimulation. Transient redistribution of state occupancy, in addition to direct modulation of transition rates, may underlie β-AR modulation of I_{Ks} time dependence.

INTRODUCTION

The delayed rectifier potassium current (I_K) accounts for the majority of repolarizing current during the action potential plateau, and its time dependence contributes to the rate-dependent shortening of action potential duration (APD). The slowly activating component of I_K, referred to as I_{Ks}, is strongly upregulated by phosphorylation through protein kinase A (PKA) (1–3), thus balancing the increase in inward current elicited by β-adrenergic stimulation of I_{CaL}. The I_{Ks} channel is constituted by four KCNQ1 proteins, which can form functional homomeric potassium channels, plus an uncertain (probably two) number of KCNE1 β-subunits (4,5). Loss of function of I_{Ks} due to KCNQ1 mutations in humans is associated with QT prolongation and a high incidence of Torsade de Pointes (TdP) ventricular tachycardia (LQT1 syndrome) (6,7). In LQT1 patients, TdP typically ensues during physical or emotional stress, conditions that involve high levels of β-adrenergic stimulation (7). Taken together, the β-adrenergic modulation of I_{Ks} and the arrhythmic consequences of LQT1 mutations strongly suggest a role of I_{Ks} in the complex pattern of current changes required to maintain repolarization stability during sympathetic activation. Because of channel kinetic properties, current amplitude during repolarization is rate-dependent. Thus, in vivo, sympathetic activation modulates repolarization currents by the concurrence of direct action on adrenergic receptors and heart-rate changes. We have shown that these two factors interact in a complex way and that their match may be crucial for repolarization stability (8). Rate-dependent increase in I_{Ks} has been generally attributed to incomplete channel deactivation during short diastolic intervals, causing rate-dependent accumulation of channels in the open state. However, this should only affect the magnitude of ''instantaneous'' I_{Ks} appearing during the action potential upstroke, a view disputed by our observation that the ''time-dependent component'' of I_{Ks} onset is mainly enhanced by fast pacing (8,9). This was tentatively interpreted as rate-dependent accumulation of channels in a nonconductive state from which activation may occur rapidly (9). This interpretation has been elegantly formalized by Silva and Rudy (10) in a numerical model of I_{Ks}. This model accurately reproduced the features of I_{Ks} rate-dependence observed under basal conditions in experiments on guinea pig myocytes.

The purpose of this work was to test whether the complex interaction between direct and rate-dependent effects of β-adrenergic modulations of I_{Ks} could be interpreted within the framework of the same kinetic model. To this aim, I_{Ks} kinetics and its adrenergic and rate-dependent modulations were evaluated in guinea-pig ventricular myocytes and subsequently used as the reference for identification of the model parameters.

The results obtained extend the applicability of the model structure proposed by Silva and Rudy (10) to a broad range of complex conditions and provide insights on the molecular

Submitted September 4, 2008, and accepted for publication February 2, 2009.

*Correspondence: antonio.zaza@unimib.it

Editor: Edward H. Egelman.

0006-3495/09/05/3862/11 $2.00

doi: 10.1016/j.bpj.2009.02.017

mechanisms potentially accounting for direct and rate-dependent adrenergic modulation of I_{Ks}.

MATERIALS AND METHODS

The presented investigation conforms to the Guide to the Care and Use of Laboratory Animals published by the U.S. National Institutes of Health (NIH publication No. 85-23, revised 1996) and endorsed by the University of Milan.§

Myocyte studies

Ventricular myocytes from Hartley guinea pigs were used within 12 h from isolation. Whole-cell I_{Ks} measurements were performed at 36°C in the presence of I_{CaL}, I_{NCX}, and I_{Kr} blockade. I_{Ks} identity was verified at the end of each experiment by checking complete elimination of time-dependent outward current upon specific I_{Ks} blockade. Information on myocyte isolation procedure, experimental solutions, and channel blockers is provided in the Supporting Material (section 1.2).

The voltage dependencies of steady-state activation, activation kinetics, and deactivation kinetics were evaluated by voltage step protocols described in the Supporting Material (section 1.2). Steady-state activation data were fitted by the Boltzmann function, from which midactivation potential ($V_{0.5}$), inverse slope factor (1/S), and asymptotic current amplitude (I_{max}) were estimated. I_{Ks} kinetics during activation was quantified by biexponential fitting of current onset during the depolarizing steps; to exclude the activation delay, the initial 2% of the time course was not considered. The faster exponential component was used to quantify the kinetics of I_{Ks} onset (τ_{act}). Pause-dependence of I_{Ks} onset kinetics was analyzed by a two-step protocol, as we have described in a previous study (8). Briefly, two activating steps (S1 and S2) were separated by a variable pause. I_{Ks} onset during S2 included an instantaneous component, followed by a time-dependent one; the time-dependent component, referred to as ''reactivation'', was fitted and its time constant (τ_{react}) was estimated as for activation (11). Dependency of τ_{react} on the S1–S2 interval, referred to as ''restitution'', was quantified by monoexponential fitting to yield the restitution time constant (τ_{rest}). The same criteria for quantification of I_{Ks} kinetics were applied for experimental and model results.

Each experimental protocol was performed in control conditions and in the presence of 0.1 μmol/L of isoprenaline (ISO), a concentration one log unit above the half-maximal effective concentration (12.9 nM) (12)). Control and ISO measurements were performed within the same myocyte, thus allowing for internal comparison.

Statistical analysis

Experimental data are presented as mean ± standard error (SE). Differences in experimental activation, deactivation and reactivation data sets between control and ISO were tested by two-way ANOVA for paired measurements (SAS/LAB software); difference was defined by significance of F statistics for either the treatment factor, or the treatment by voltage interaction. Curve fitting was performed by the least-square method (Origin Microcal 7.0); goodness of fitting was tested by the chi-square test on correlation coefficients (R). Differences between parameter means were tested by Student's t-test for paired measurements, and with post-hoc analysis (SAS/LAB software) in the case of multiple comparisons. Sample size for each protocol is reported in the respective figure legend.

In the analysis of myocyte experiments, curve fitting was performed on data from individual cells and results are reported as the mean ± SE of parameter estimates; in this case, differences between curves were tested by comparing parameter populations. To obtain a reference for model optimization, curves fitted on averaged myocyte data points were also obtained. Parameters from ''average'' experimental curves (reported without SE) were used only to provide a quantitative comparison with model-generated curves. Parameters obtained by fitting an average curve may differ slightly from the mean of individual cell parameters.

Computational analysis

The Markov model structure (Fig. S1) implemented in this study was derived by Silva and Rudy (10). It describes the properties of I_{Ks}, including all of its KCNQ1 and KCNE1 subunits, by means of 15 closed states to account for four independent voltage sensors, each undergoing two conformational changes before channel opening. The group of closed states representing channels for which the first transition has been completed by only part of the four voltage sensors is called ''Zone 2''. The group of closed states representing channels in which the first transition has been completed by all four voltage sensors is called ''Zone 1''. There are two open states. The whole-cell I_{Ks} current is given by:

$$I_{Ks} = G_{Ks} \times P_O \times (V - E_{Ks}), \quad \text{where}$$
$$G_{Ks} = \sigma \times g_{Ks}. \qquad (1)$$

The variable P_o represents the sum of the probabilities of occurrence in the open states, V is the membrane potential, and E_{Ks} is the K^+ reversal potential. G_{Ks} is the maximum membrane conductance obtained as the product of channel density (σ) and the unitary channel conductance (g_{Ks}). E_{Ks} was set to −72.4 mV, as measured in preliminary experiments (8). G_{Ks} was set to 12 nS and remained unchanged under ISO stimulation. G_{Ks} dependence on changes in cytosolic Ca^{2+} was neglected, because ISO modulation of I_{Ks} gating was analyzed under conditions ruling out its contribution (with both I_{CaL} and I_{NCX} blocked).

The expressions describing transition rates between channel states and their parameters are reported in Tables S1 and S2. Parameter identification was based on model optimization versus experimental data, as described in the Supporting Material (section 1.3). MATLAB 7 and Simulink (The MathWorks, Natick, MA) were used for all the numerical computations.

Implementation of previous Hodgkin-Huxley-type models

To test whether alternative models could reproduce specific I_{Ks} features such as pause-dependence (also referred to as ''restitution'') of reactivation rate, we implemented the formulations proposed by Terrenoire et al. (13) and by Imredy et al. (12), respectively. The two models were applied (with their original parameter values) to compute I_{Ks} and its modulation by ISO in the S1–S2 protocol. This section, presented in detail in the Supporting Material (section 2.2), is summarized here.

Action potential simulations

The effect of 100 nM ISO was simulated by modulation of I_{Ks} (according to presented results), I_{CaL} (scaled by a factor of 1.5), and rate of Ca^{2+} uptake by the sarco/endoplasmic reticulum Ca^{2+}-ATPase (SERCA) flux scaled by a factor of 1.5. Changes in conductances other than I_{Ks} were required, because I_{CaL} directly contributes to APD and SERCA flux can indirectly affect the Na^+/Ca^{2+} exchanger current. In the case of I_{CaL}, simple scaling is an approximation of PKA-dependent modulation, which also involves shifts in activation and inactivation voltage dependency (14), but may be adequate for our purposes.

RESULTS

I_{Ks} properties in myocytes under control conditions

Voltage dependence of I_{Ks} gating properties measured from myocytes in control is illustrated by open symbols in Figs. 1 and 2; sample current records are shown in Fig. S2. Boltzmann fitting of steady-state activation curves of individual cells yielded $V_{0.5} = 26.6 \pm 2.5$ mV, $1/S = 12.0 \pm 0.7$ mV,

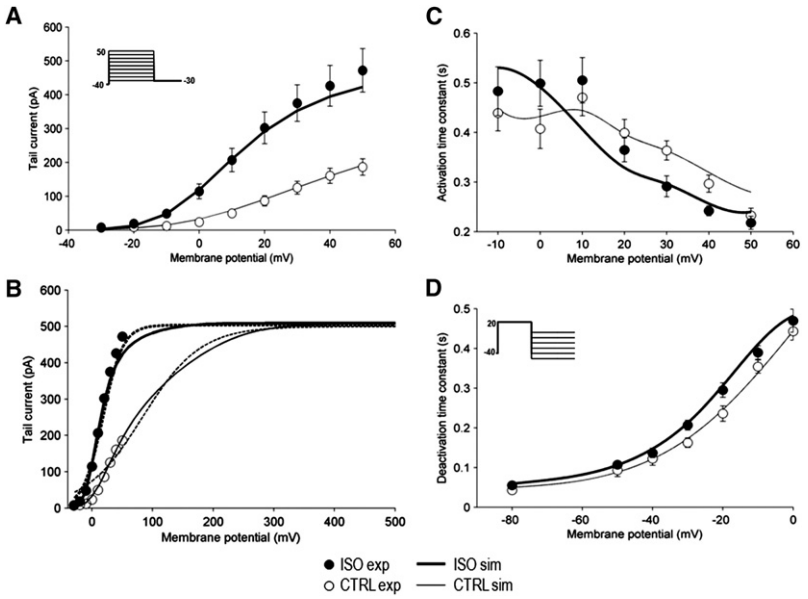

FIGURE 1 ISO effect on voltage dependence of I_{Ks} gating. Experimental data (mean ± SE) shown by symbols (control: *open symbols*; ISO: *solid symbols*); model simulations by lines (control: *thin lines*; ISO: *thick lines*). (*A*) Steady-state activation ($n = 15$). (*B*) Extension of steady-state activation simulations over a wider range of potentials (experimental *data points* as in A superimposed for comparison); dotted lines represent Boltzmann fitting of simulated data. (*C*) Activation kinetics ($n = 15$); (*D*) Deactivation kinetics ($n = 16$). Voltage protocols in inset.

and $I_{max} = 197 \pm 26$ pA. However, even at the most positive potential tested, steady-state current failed to show clear-cut saturation in most of the experiments; thus, the parameters estimated by Boltzmann fitting should be interpreted with caution and are reported here only for comparison with previous work.

The time constant of the fast component of I_{Ks} activation (τ_{act}, Fig. 1 *C*) remained unchanged between 0 and 10 mV and decreased between 10 and 50 mV. Deactivation time constant (τ_{deact}, Fig. 1 *D*) decreased monotonically with membrane hyperpolarization. At 0 mV, deactivation rate did not differ significantly from activation rate ($\tau_{deact} = 443 \pm 22$ ms; $\tau_{act} = 407 \pm 39$ ms, NS).

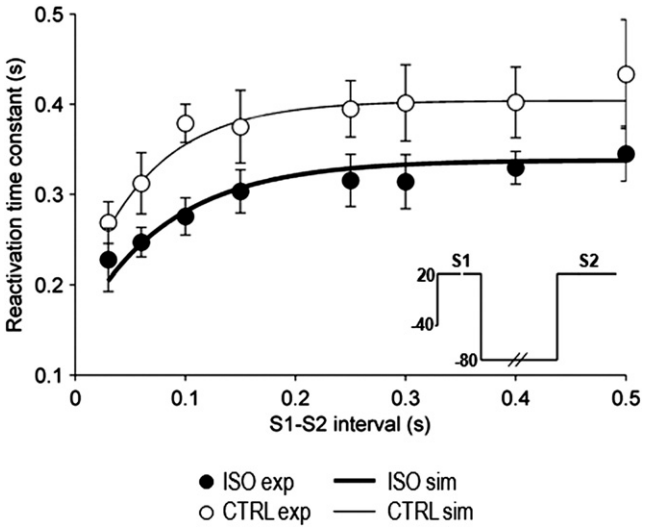

FIGURE 2 ISO effect on I_{Ks} reactivation kinetics and its pause-dependence (restitution, $n = 5$). Reactivation time constants (τ_{react}) are plotted versus S1–S2 intervals. Meaning of symbols and lines as in Fig. 1. Experimental data points from Rocchetti et al. (8).

The reactivation of I_{Ks}, analyzed by the S1–S2 protocol, was composed of a time-independent (instantaneous) component and a time-dependent one (Fig. S2 *C*). As the S1–S2 interval was shortened, the instantaneous component of I_{Ks} activation during S2 increased, with a time course reflecting channel deactivation at –80 mV. The time constant (τ_{react}) of the time-dependent component increased as S1–S2 was prolonged. The dependency of τ_{react} on S1–S2 (Fig. 2) was fitted by a single exponential, with a time constant (τ_{rest}) of 68.5 ms and an asymptotic value of τ_{react} of 411 ms. Because reactivation after a sufficiently long S1–S2 interval is equivalent to activation from resting conditions, the asymptote of τ_{react} was similar to that of τ_{act} at the same membrane potential (20 mV, $\tau_{act} = 399$ ms).

Model identification under control conditions

As described in the Supporting Material (section 1.3), the Markov model (Fig. S1) was optimized to reproduce all the experimental results in control by a single set of parameters. Model simulations of gating voltage dependence in control are shown in Figs. 1 and 2 by thin lines (symbols omitted for clarity); simulations of sample I_{Ks} records are shown in Fig. S2. Within the voltage range tested experimentally (≤ 50 mV), the simulated steady-state activation curve visually overlapped the data (Fig. 1 *A*); indeed, Boltzmann fitting of simulated points ($R^2 > 0.99$) yielded parameters similar to those obtained by fitting mean experimental values ($V_{0.5} = 25.6$ vs. 25.6 mV, inverse slope factor = 14.6 vs. 13.0 mV, and asymptote = 231 vs. 215 pA.). However, extension of simulations to potentials beyond 50 mV showed a further increase in steady-state current, which achieved a saturation value (I_{max}) of 509 pA at much more positive potentials (Fig. 1 *B*). Interestingly, the Boltzmann function could not be adequately fitted to the extended activation curve predicted by the model (Fig. 1 *B*), even if no constraint was put on parameter estimation.

Simulated voltage dependence of τ_{act} was consistent with that of experimental data (Fig. 1 *C*), even if τ_{act} was overestimated at 50 mV. Voltage dependence of τ_{deact} was accurately reproduced by simulations over the wide range of membrane potentials tested (Fig. 1 *D*).

As shown in Fig. 2, I_{Ks} reactivation and its restitution were also well predicted by the model; exponential fitting of simulated restitution ($R > 0.93$) yielded a τ_{rest} of 62.9 ms and an asymptotic τ_{react} of 406 ms, with both values similar to those measured in myocytes (68.5 ms and 411 ms, respectively).

To summarize, except for minor quantitative inaccuracy in the prediction of activation rate, the model reproduced I_{Ks} gating features examined by all of the protocols. Such a stringent validation confirms the adequacy of the I_{Ks} model structure proposed by Silva and Rudy (10).

I_{Ks} properties in myocytes during β-adrenergic stimulation

Voltage dependency of I_{Ks} gating properties measured from myocytes during exposure to ISO is illustrated by solid symbols in Figs. 1 and 2; sample current records are shown in Fig. S2. β-receptor stimulation by ISO markedly increased I_{Ks} amplitude (Fig. 1 *A*), with smaller but significant effects on its kinetics (Fig. 1, *C* and *D*).

Boltzmann fitting of steady-state activation curves of individual cells yielded a $V_{0.5}$ of 15.7 ± 1.9 mV, a 1/S of 11.9 ± 0.6 mV, and an I_{max} of 464 ± 62 pA. A significant difference was found for I_{max} (266 ± 34% of control; $p < 0.05$; Fig. 1 *A*) and $V_{0.5}$ ($\Delta = -10 \pm 2.2$ mV; $p < 0.05$) between ISO and control. However, as in control conditions, also in the presence of ISO, steady-state current failed to show clear-cut saturation.

The voltage dependence of activation time constant (τ_{act}, Fig. 1 *C*) was slightly rotated clockwise by ISO, thus resulting in a slowing of activation between 0 and 10 mV and acceleration between 10 and 50 mV ($p < 0.05$ for voltage by treatment interaction in ANOVA).

Deactivation was slowed by ISO (Fig. 1 *D*, $p < 0.05$ for treatment in ANOVA). In particular, τ_{deact} was increased by a maximum of 59 ms at −20 mV ($p < 0.05$); at diastolic potential (−80 mV), τ_{deact} was 43 ± 2.5 ms in control and 55 ± 2.9 ms with ISO (NS).

Exponential fitting of the restitution of τ_{react} (Fig. 2) yielded an asymptotic τ_{react} of 339 ± 8 ms ($p < 0.05$ versus control) and a τ_{rest} of 132 ± 30 ms (192% of control; $p < 0.05$). Thus, ISO significantly accelerated reactivation at all S1–S2 intervals ($p < 0.05$ for treatment in ANOVA) and slowed the restitution process, thereby extending its influence to a wider range of diastolic intervals.

I_{Ks} model identification during β-adrenergic stimulation

ISO effects detected in myocytes were reproduced, within the same model structure used in control, by adjusting the parameters governing the transitions between channel states (Fig. 3). The G_{max} parameter (see Eq. 1) was deliberately kept constant to test the hypothesis that its change is theoretically unnecessary to account for I_{Ks} response to ISO. The ground for such a hypothesis is discussed in the detail in the Supporting Material (section 3.2).

Simulations of gating voltage dependence in ISO are shown in Figs. 1 and 2 by thick lines (symbols omitted for clarity); simulations of sample I_{Ks} records are shown in Fig. S2. Boltzmann fitting of the simulated steady-state activation curves during ISO yielded a $V_{0.5}$ of 10.3 mV (−15.3 mV versus control), 1/S of 12.1 mV (−2.5 mv versus control), and an I_{max} of 436 pA (188% of control). These parameters should be compared with those obtained by fitting mean experimental values, which estimated ($R^2 > 0.99$) a $V_{0.5}$ of 14.2 mV (−11.4 mV versus control), a 1/S of 11.9 (−1.1 mV versus control), and an I_{max} of 484.1 pA (225% of control). Thus, when analyzed by Boltzman fit over the physiological range of potentials, modeled and experimental data consistently indicated that ISO increased I_{max} and shifted $V_{0.5}$, without changing 1/S. However, when simulations were extended to potentials beyond 50 mV, the same I_{max} value was achieved in ISO and control (509 pA, Fig. 1 *B*), ISO markedly increased the steepness of the activation curve (i.e., substantially reduced 1/S), and its Boltzmann fitting, although not yet optimal, was considerably improved compared with that obtained in control (Fig. 1 *B*).

In the voltage dependence of τ_{act} (Fig. 1 *C*), the crossover between control and ISO curves was reproduced by simulation;

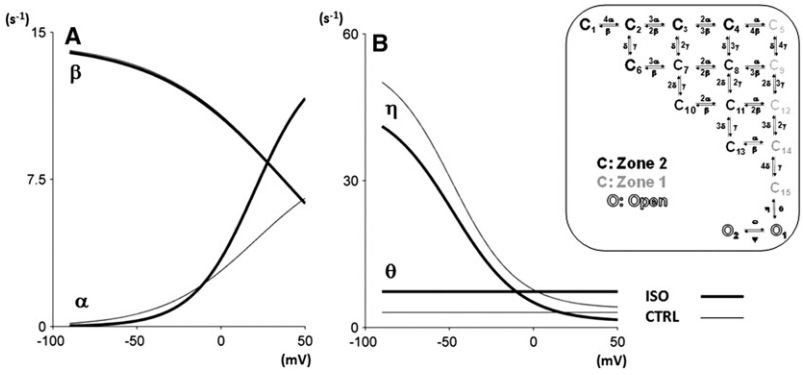

FIGURE 3 Changes in the voltage dependence of model transition rates (see *schematic* on the right) required to model ISO effects. (*A*) Zone 2 forward (α) and backward (β) transition rates. (*B*) Opening (θ) and closing (η) transition rates. Thin lines for control conditions; thick lines for ISO. Transitions rates unaffected by ISO not shown for simplicity.

however, it occurred at a slightly more negative potential than that occurring in experiments. On the other hand, the voltage dependency of τ_{deact} was also well reproduced by the model in quantitative terms (Fig. 1 *D*). The model also succeeded in reproducing the complex effect of ISO on I_{Ks} reactivation rate and on its restitution process (Fig. 2). Exponential fitting of simulated τ_{react} restitution curves yielded an asymptotic τ_{react} of 338 ms (83% of control) and a τ_{rest} of 107 ms (169% of control). Whereas estimates of ISO-induced changes were qualitatively correct, the increase in τ_{rest} was slightly underestimated by the model (169% vs. 192%).

Overall, the model was able to qualitatively reproduce all ISO effects, with minor quantitative differences. We then proceeded to identify which transitions in the kinetic scheme (Fig. S1) were crucial in modeling ISO effects.

Model-based analysis β-adrenergic modulation of channel kinetics

As illustrated in Fig. 3, model optimization to reproduce ISO effects resulted in modification of only few among the transition rates of the Markov model, namely α, θ, and η. For each channel monomer, the changes resulted in facilitation of the transition between the first and the second closed state (α increased for $V > -20$ mV, β minimally affected) and of the final opening transition (θ increased, η decreased). The second voltage-dependent transition (rates γ and δ) and the transition between the two open states (rates ψ and ω), were not modified in reproducing ISO effects.

ISO effects on I_{Ks} were first analyzed in steady-state conditions by observing the distribution of state occupancy at different voltage levels (Fig. 4). At resting potential (-80 mV, Fig. 4 *A*), channels almost exclusively resided in Zone 2, and, up to -40 mV (not shown), ISO minimally affected the occupancy distribution. Upon small depolarization beyond threshold (e.g., 0 mV, Fig. 4 *B*), ISO increased open-state occupancy at the expense of Zone 2 occupancy, with Zone 1 remaining almost unchanged. At mid-activation potential (20 mV, Fig. 4 *C*), ISO induced a strong shift from all closed states toward the open ones. For depolarization to 50 mV (Fig. 4 *D*) in control conditions, the occupancy of closed states (mainly Zone 1) was still substantial (0.6). This situation was dramatically changed by ISO, which caused almost complete channel opening.

The effect of ISO on the dynamic evolution of state occupancies is analyzed in Figs. 5–8. To this end, simulations were run

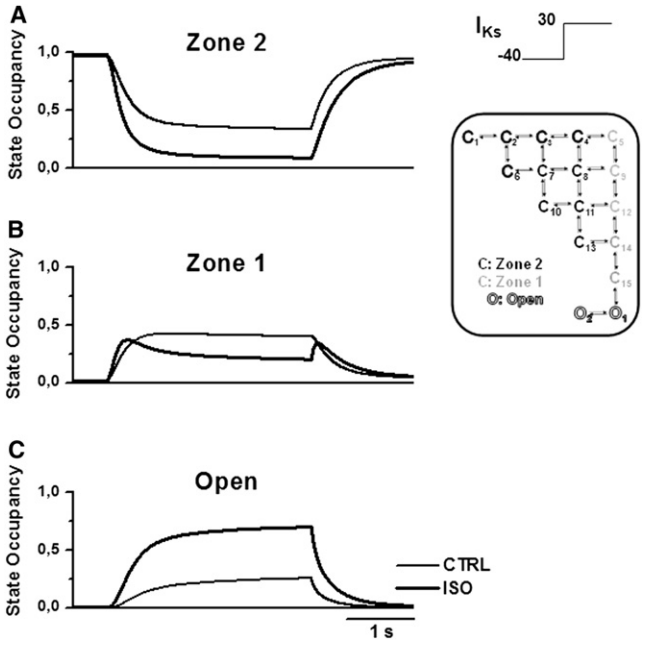

FIGURE 5 Model analysis of I_{Ks} activation course during a V-step protocol (*inset*) in control (*thin lines*) and in ISO (*thick lines*). (*A*) Zone 2 occupancy. (*B*) Zone 1 occupancy. (*C*) Open-state occupancy.

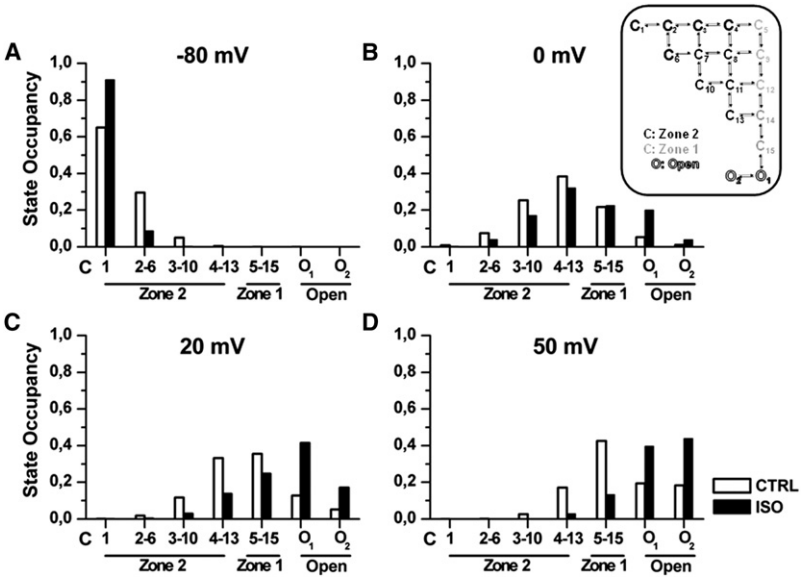

FIGURE 4 Steady-state distribution of model states occupancy at selected potentials. (*A*) -80 mV = diastolic. (*B*) 0 mV. (*C*) +20 mV ≅ 50% activation. (*D*) +50 mV ≅ 95% activation in control (*open bars*) and in ISO (*solid bars*). States (see *schematic* on the right) are represented on the abscissa from those farther (*Zone 2*) to those closer (*Zone 1*) to channel opening (*open*). State occupancy is defined as (*n* of channels in a state)/(total *n* of channels).

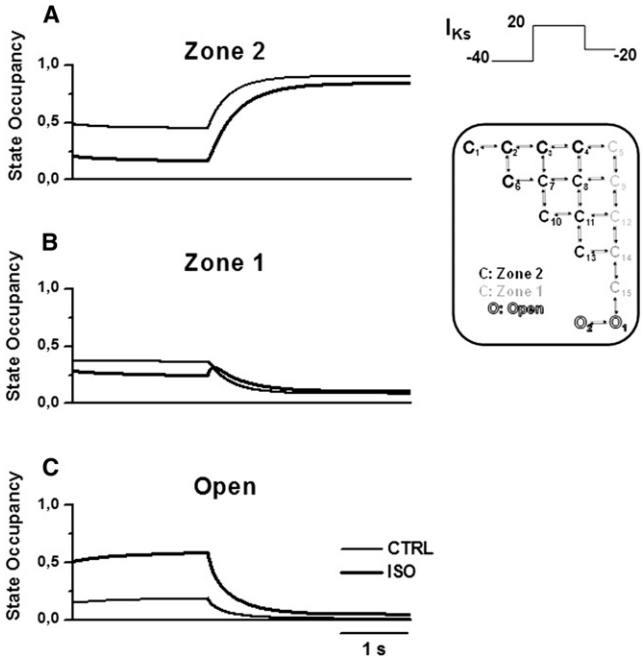

FIGURE 6 Model analysis of I_{Ks} deactivation course during a V-step protocol (*inset*) in control (*thin lines*) and in ISO (*thick lines*). Panels as in Fig. 5.

for conditions maximizing differences between control and ISO (activation $V_{test} = 30$ mV; deactivation $V_{test} = -20$ mV: reactivation S1–S2 interval = 100 and 500 ms).

During activation (Fig. 5), ISO increased the amount and the velocity of channels exiting Zone 2, thus promoting transient accumulation of channels in Zone 1 (Fig. 5 *B*). Furthermore, ISO facilitated the opening transition (Fig. 5 *C*). The two effects cooperated in accelerating I_{Ks} onset during activation and led to the opening of the majority of channels. Indeed, after 3 s at 30 mV, 70% of channels opened with ISO compared with 26% in control (Fig. 5 *C*).

ISO-induced slowing of I_{Ks} deactivation was analyzed by simulating repolarization to −20 mV from steady-state activation at 20 mV (Fig. 6). In control conditions, repolarization caused channels to move rapidly from open states, through Zone 1, to Zone 2 (Fig. 6). In the presence of ISO, the flow of channels from open states with increased occupancy met the bottleneck generated by the slow Zone 1–Zone 2 transition. This factor led to a transient accumulation of channels in Zone 1 (Fig. 6 *B*), which was a hindrance to the transition of channels from the open to a nonconductive state. Thus, albeit directly slowed by ISO (smaller η; see Fig. 3), the closing transition may not represent the only rate-limiting factor for deactivation in this scheme.

I_{Ks} pause-dependence (representative of rate-dependence) and its modulation by ISO were analyzed by comparing effects on reactivation at short (100 ms, Fig. 7) and long (500 ms, Fig. 8) S1–S2 intervals. During the S1–S2 interval, channels migrate from the open states to Zone 1 and Zone 2, sequentially. As suggested by Silva and Rudy (10), with shorter S1–S2 intervals reactivation during S2 was faster because of incomplete return to Zone 2 (cf. Fig. 7 *B* with Fig. 8 *B*); this decreased the proportion of channels requiring two transitions before opening. ISO enhanced the rate-dependence of I_{Ks} instantaneous component and of reactivation rate, respectively, by different mechanisms. The former effect was very small and occurred because of slight deactivation slowing at −80 mV, which prolonged persistence in the open state at short S1–S2 intervals (Figs. 7 *D* and 8 *D*). In myocytes ISO mainly affected reactivation rate in two ways: it decreased the steady-state value of τ_{react} and slowed the time course by which the steady-state was achieved (increased τ_{rest}). Steady-state reactivation is in fact equivalent to activation; thus, ISO effects on steady-state τ_{react} and on τ_{act} (at 20 mV) were unsurprisingly similar and were explained by the same mechanism (see above). A more complex mechanism accounted for the rate-dependent effect of ISO on τ_{react}. Fig. 7 *C* shows that, in the presence of ISO (*thick line*), Zone 1 occupancy during the S1–S2 interval transiently increased above the value achieved during S1. This increased the proportion of channels available for direct opening during S2. In turn, the ISO-induced increase in Zone 1 occupancy during the S1–S2 interval was the consequence of the large increase in open-state occupancy during S1 (Fig. 7 *D*, *thick line*). This interpretation was tested in the model by introducing ISO-induced gating changes only at the beginning of the S1–S2 interval. Under this condition (Figs. 7 and 8, *dashed line*), probability of open-state occupancy was not increased during S1, no Zone 1 channel accumulation occurred during the S1–S2 interval (in Fig. 7 *C*, *dashed line* initially overlaps with *control line*), and reactivation during S2 was slower than that achieved when ISO was applied throughout the entire protocol (Fig. 7 *A*, cf. *dashed* and *thick lines*). The dashed-line reactivation was still faster than the control one (Fig. 7 *A*, *thin line*) because of pause-independent (i.e., steady-state) ISO effect on τ_{react}. The difference in reactivation rate between the thick and dashed lines in Fig. 7 *A* represents the pause-dependent component of ISO effect, which accounts for the slowing in the restitution process. Indeed, Fig. 8 *C* shows that, at long S1–S2 intervals, ISO-induced channel accumulation in Zone 1 dissipates before reaching S2, thus leading the thick and dashed lines to overlap during reactivation (Fig. 8 *A*).

Comparison with reactivation kinetics in Hodgkin-Huxley-type models

A comparison of I_{Ks} reactivation between the presented and HH-type models is shown in Fig. S3. The model by Terrenoire et al. (13) included three independent but identical gates. Some pause-dependence of reactivation rates could be generated by such formulation, but it did not reproduce experimental observations, because the time range of restitution was too narrow and insensitive to ISO. This is because pause-dependence of reactivation rate required diastolic

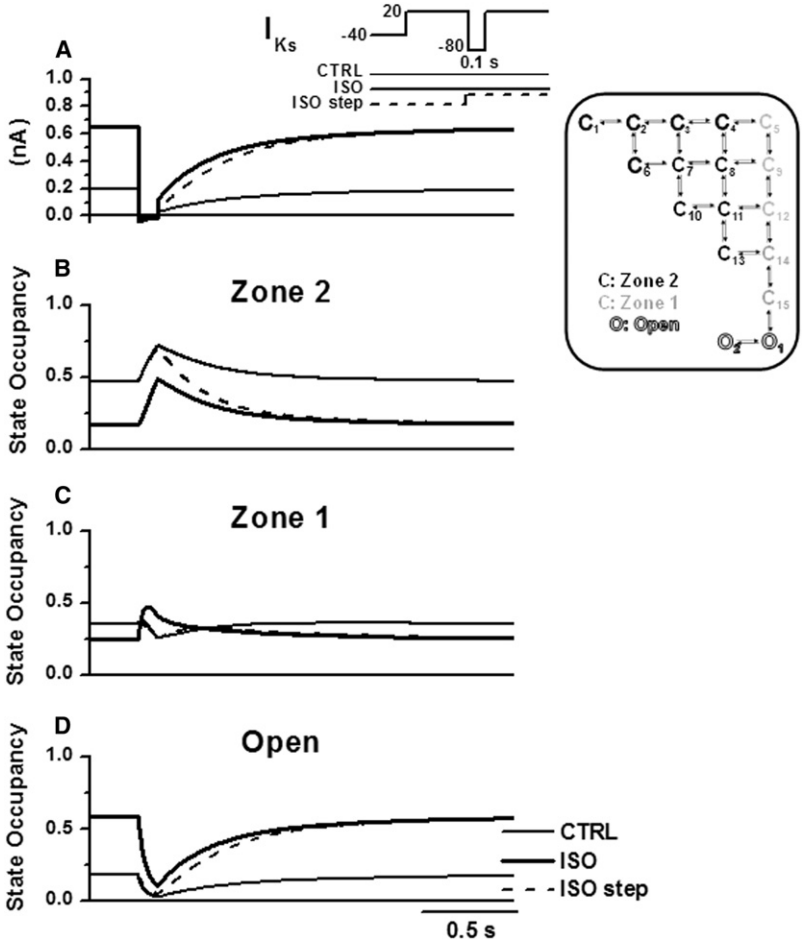

FIGURE 7 Model analysis of I_{Ks} reactivation at a short S1–S2 interval (100 ms) in control (*thin line*) and in ISO (*thick line*). Voltage protocols in inset. The dashed line shows the effect of ISO applied after S1 (*"ISO step" in inset*). (*A*) Current (I_{Ks}). (*B*) Zone 2 occupancy. (*C*) Zone 1 occupancy. (*D*) Open-state occupancy.

deactivation to be incomplete at the time of S2; therefore, modulation of residual activation was constrained by the small effect of ISO on τ_{deact} at −80 mV (Fig. 1 *D*). This explains why, although Terrenoire's formulation may in principle accommodate restituition of reactivation rates, it cannot reproduce experimental observations (Fig. S4).

Imredy's formulation (12) failed to reproduce reactivation pause-dependence (Fig. S4). In this model, gating was simulated by the product of two gating components with independent and strongly different kinetics. Reactivation pause-dependence could not be reproduced at all because of the specific formulation of the gating components. Even if pause-dependence of reactivation rate could be reproduced in this model, it would still rely on incomplete diastolic deactivation.

In summary, depending on the specific formulation, Hodgkin-Huxley (H-H)-type models may incorporate pause-dependence of reactivation rate in principle; nevertheless, they cannot reproduce experimental data in terms of magnitude and response to ISO. This is mainly because, in H-H models, pause-dependence of reactivation rate depends uniquely on incomplete diastolic deactivation (i.e., gating variables $>$ 0 at the onset of S2), which strictly constrains the model output. This is not the case for Markov models, in which redistribution between sequential closed states can contribute to explain the phenomenon. The results obtained with Terrenoire's and Imredy's models are illustrated and discussed in further detail in the Supporting Material (section 2.2).

Action potential simulations

In guinea-pig myocytes, ISO causes counterclockwise rotation of the relationship between APD and stimulation cycle length (CL) (8), with convergence of control and ISO relationships at a CL of 0.15 s. To test the performance of modeled I_{Ks} in simulating such an effect, we incorporated the presented I_{Ks} formulation in an action potential model (10,15). Under control conditions, the model generated an APD/CL relationship comparable to that observed in guinea pig myocytes, and incorporation of ISO-induced changes reproduced its counterclockwise rotation (Fig. S5). The model-generated control and ISO relationship converged at a CL of 0.7 s, which was significantly longer than the CL observed experimentally. ISO modulation of APD reflected the balance between the opposite effects of I_{CaL} and I_{NCX} enhancement on one side and I_{Ks} enhancement on the other. The CL at which opposite contributions balance each other is highly sensitive to their relative magnitudes and rate-dependence. Therefore, modulation of I_{CaL} and SERCA other than

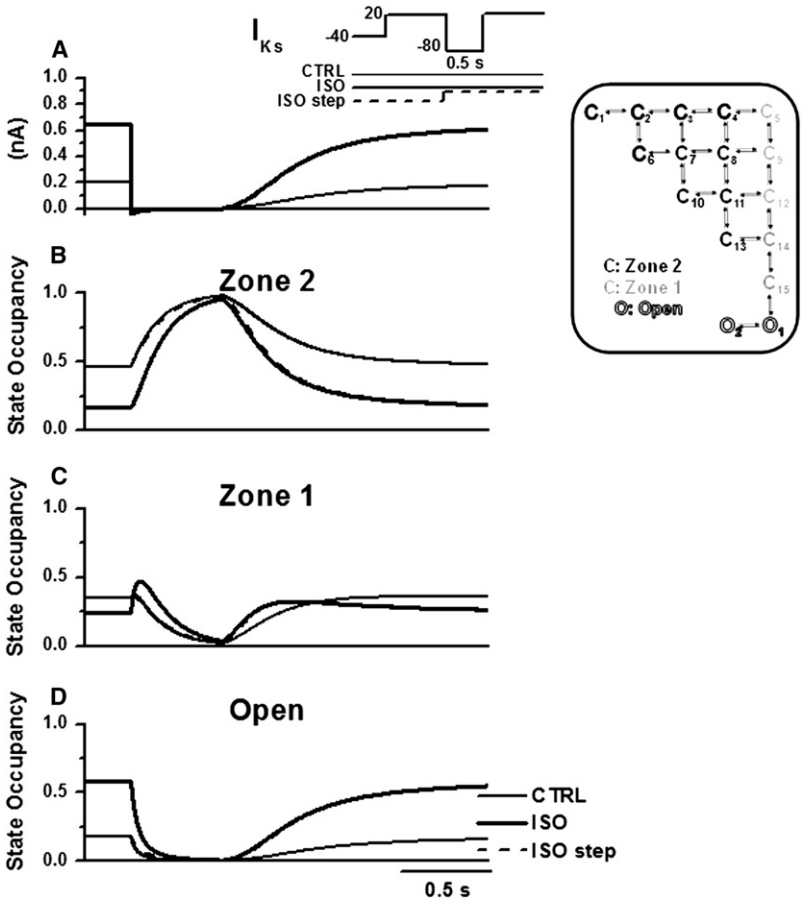

FIGURE 8 Model analysis of I_{Ks} reactivation at a long S1–S2 interval (500 ms). Protocol and legends as in Fig. 7.

arbitrary scaling may be required to achieve quantitatively accurate simulation of ISO effects.

β-adrenergic stimulation was then reproduced in the presence of a 50% reduction in I_{Ks} maximal conductance (Fig. S5). In this case, counterclockwise rotation was accompanied by an upward shift of the whole APD/CL relationship and, at CL $\geq$ 1.5 s, repolarization failed. The effect of such partial I_{Ks} reduction was large compared with that of repolarization abnormalities in human long QT syndromes with almost complete loss of I_{Ks} function (16). Such a difference may reflect the larger role of I_{Ks} in guinea-pig repolarization, for which the action potential model was developed.

DISCUSSION

The presented experimental results extensively describe I_{Ks} gating properties in guinea-pig myocytes and their modulation by ISO. In model simulations all baseline I_{Ks} features could be reproduced by a single set of kinetic parameters and ISO-induced effects were reproduced, within the same model structure, by changes in the parameters governing selected transitions. Analysis of the model adjustments necessary to reproduce ISO effects leads to several ''inferential'' conclusions on the modulation of I_{Ks} gating by β-AR stimulation.

I_{Ks} properties in myocytes

PKA-dependent modulation of I_{Ks} gating properties were previously described in heterologously expressed human channels and native guinea-pig myocytes (13,17). The purpose of our experiments was to fully characterize gating of native I_{Ks} and its β-adrenergic modulation under strictly uniform conditions, as necessary in developing and testing a comprehensive model with quantitative accuracy.

A feature of I_{Ks} consistently observed in this and in many other studies (3,18,19) is failure of its steady-state activation to saturate within the range of potentials that can be tested experimentally in myocytes (<50–60 mV), and up to 120 mV in heterologous KvLQT1/IsK (20). In the absence of clear-cut saturation, I_{max} estimation by Boltzmann fitting is arbitrary; regardless, adrenergic modulation of I_{Ks} activation is routinely analyzed in terms of changes in parameters estimated from Boltzmann fitting. When such an approach was applied to the data, ISO effect on steady-state activation consisted of a large increase in I_{max} and a smaller negative shift of $V_{0.5}$, which is in line with previous findings. Extension of steady-state activation analysis to a wider range of potentials by model simulations suggests that this approach might be misleading (see section on model-based analysis of adrenergic modulation, below). Thus, ISO-induced changes

in Boltzmann parameters should not be interpreted mechanistically.

ISO increased activation rate and slightly slowed deactivation rate. ISO-induced changes in I_{Ks} dependency on interpulse interval included an increase of reactivation rates and a slowing of their restitution. Consistent with the nonsignificant effect of ISO on I_{Ks} deactivation rate at -80 mV ($\Delta\tau_{deact} = +12$ ms at -80 mV), pause-dependence of I_{Ks} instantaneous component was almost unaffected. Faster reactivation may partly reflect ISO-induced acceleration of activation rate; however, at short S1–S2 intervals, reactivation (in S2) was accelerated more than activation (in S1), and the restitution course was also affected.

This complex pattern of changes provides highly stringent conditions for testing any kinetic scheme; thus, the performance of the relatively simple model applied in this work was almost surprising. In light of this, the gating mechanisms suggested by model simulations, albeit theoretical, deserve to be considered in detail.

Mathematical model of I_{Ks}

To encompass the wide spectrum of I_{Ks} properties tested in the presented study, we adopted a Markov-type model structure, previously demonstrated by Silva and Rudy (10) to adequately reproduce I_{Ks} complex features under baseline conditions. Several features of our control data were not correctly reproduced using the parameters published by Silva and Rudy (10), which resulted in excessive maximal conductance, slow deactivation rates (especially for $Vm > -50$ mV), and unsatisfactory fitting of the pause-dependence of reactivation rates (restitution). This may result from quantitative differences between the presented results and those of Lu et al. (21), used as a reference for parameter optimization by Silva and Rudy (10).

The single set of parameters identified by the optimization procedure was adequate to reproduce all I_{Ks} features observed under baseline conditions. The voltage dependence of steady-state activation predicted by the model could not be fitted by a Boltzmann function, even if no constraint was put on its parameters. This observation can be interpreted in terms of channel kinetics. Indeed, because a Boltzmann function describes a single transition between closed and open states, it may not be adequate to model multiple sequential transitions over the whole range of activation voltages. In terms of I_{Ks} dynamic behavior, the presented results lead to the relevant conclusion that interpretation of pause-dependence of reactivation rates can be effectively explained by redistribution of channels to states nearer to the open one within a single chain of Markov states (i.e., no requirement of transition between different gating modes). A more detailed discussion of I_{Ks} gating features relevant to its modeling is also provided in the Supporting Material (section 3.1).

Modeling of β-adrenergic I_{Ks} modulation has been previously addressed by H-H-type formulations, in which I_{Ks} kinetics were represented by the product of multiple (2 (12,22) or 3 (13) identical (13,22) or nonidentical (12)) gating variables, as required to reproduce the initial lag in current activation. However, it was unclear to what extent these models could reproduce the complex pause-dependence of I_{Ks} reactivation rate, a feature observed for both heterologously expressed human channels (11) and native ones (9) and modulated by β-adrenergic receptors (8). This issue was addressed by implementing previous H-H-type models and applying them to the presented experimental data. This analysis showed that, although H-H models can in principle reproduce pause dependence of reactivation rate, failure to consider sequential (not independent) transitions between closed states strictly constrains their output, thus making it unsuitable to match experimental observations. The presence of sequential transitions for the activation of each independent KCNQ1 subunit, such as those implemented in the presented model, are suggested by experimental evidence (23). The presented results support the concept that sequential gating may be necessary to account for I_{Ks} kinetic behavior and its modulation.

Model-based analysis of I_{Ks} β-adrenergic modulation

According to Boltzmann analysis, the most prominent effect of ISO consists in a large increase in I_{max} (Fig. 1 *A*). In previous models (13,22), such an increase was reproduced by an increment in the term G_{Ks} of Eq. 1, which implies an increase in g_{Ks}, in channel density (σ), or both.

To our best knowledge, modulation of g_{Ks} by protein phosphorylation has been described exclusively in nonvoltage-gated channels (gap-junctions, AMPA-R, RyR) (24–26), whereas the possibility of ISO-induced changes in g_{Ks} has not been experimentally tested because of difficulties in recording I_{Ks} single-channel currents. On the other hand, modulation of σ might occur with a time course roughly compatible with the response of I_{Ks} amplitude to ISO (27), but it would not account for changes in the voltage dependence of current kinetics (for detailed discussion see the Supporting Material, section 3.2). These considerations motivate the interest in testing the unitary interpretation that all ISO effects on I_{Ks} may be mediated by changes in channel P_o.

Model fitting to data points under control conditions identified a set of gating parameters that estimated an open probability of 0.4 at 50 mV, the most positive potential experimentally tested; maximal conductance was achieved only at potentials exceeding the physiological range. According to this interpretation, the apparent ISO-induced increase in I_{max} was instead a simple increased P_o within the range of potentials tested, and may reflect enhanced sensitivity of the activation gating to membrane depolarization. In this context, I_{Ks} ''reserve'' available to recruitment through receptor stimulation would amount to 60% of the total channel population and correspond to the fraction of channels still residing in Zones 2 and 1 during depolarization at 50 mV (Fig. 4). The

magnitude of available reserve identified by our results is far larger than that predicted by the original Silva and Rudy model (10). Indeed, simulations carried out with their parameters (not shown) resulted in more than 90% of channels being open upon depolarization at 50 mV under baseline conditions. This implies that a biologically implausible increase in G_{Ks} would still be required in the original model formulation to account for the large effect of ISO on maximal steady-state current. Nevertheless, such a limitation was overcome in the presented study by acting exclusively on transition rates, thus proving that the Silva and Rudy kinetic scheme (10) can accommodate a wider range of observations. Interestingly, the Boltzmann function fitted the predicted activation curve much better in ISO than in control (Fig. 1 *B*). This may result from an apparent lumping of sequential closed-state transitions, resulting from the steeper voltage dependence of their rates (α-parameter, Fig. 3 *A*).

The effects of ISO on the complex time-dependent behavior of I_{Ks} were also well reproduced by the model. The opening transition rate was directly modulated by ISO; however, a relevant feature underlying ISO effects on current time course after membrane potential changes was transient ''accumulation'' of channels in states near to the open one (Zone 1). By analogy with the concentration of reactants in a chemical reaction, such an accumulation contributes to determine the flow of channels between states. Transient changes in occupancy are, in turn, the consequence of modulation of transition rates. However, the latter may be far more complex than is direct modulation of channel opening; indeed, a change in occupancy may reflect the net balance between effects on multiple transitions, including those between nonconductive states. In terms of channel structure, this implies that stabilization at diastolic potential of a conformation corresponding to an intermediate closed state might paradoxically increase the kinetics of current onset during activation.

Study limitations

The guinea pig was chosen as the animal model for this analysis because it has a robust I_{Ks} expression even under baseline conditions; moreover, the original model formulation was developed for this species. However, important differences in I_{Ks} expression level and kinetics exist between the guinea pig and larger mammals (dog and man) (3,28,29); therefore, these observations may not directly extrapolate to those species.

Parameter optimization was performed on several mutually independent I_{Ks} properties; this should minimize the number of suitable parameters combinations. Still, the procedure of nonlinear optimization does not guarantee uniqueness of the identified parameters in generating a set of current properties. Thus, interpretation of ISO effects, as is always the case for modeling studies, is subject to uncertainty. Moreover, in terms of mechanistic interpretation, modeling only proves that a given degree of complexity can reproduce the observed behavior, but it does not rule out more complex mechanisms.

Because we focused this study on β-adrenergic modulation of I_{Ks} gating, results on action potential simulations should only be considered as preliminary. Indeed, a more accurate modeling of β-AR modulation of cellular targets other than I_{Ks} would be necessary to predict in quantitative terms the impact of I_{Ks} modulation on whole-cell electrophysiological function.

CONCLUSIONS

The presented results show that the full complexity of I_{Ks} kinetics and of its β-AR modulation can be accounted for by the relatively simple kinetic scheme proposed by Silva and Rudy (10). Because the study was performed on native I_{Ks}, the modeled behavior is the one resulting from all channel α- and β-subunits considered as a functional unit. Model analysis of ISO effects provides a novel putative interpretation of agonist-induced changes in maximal channel conductance and highlights the importance of redistribution of state occupancy in determining I_{Ks} time dependence.

SUPPORTING MATERIAL

Two equations, two tables, and five figures are available at http://www.biophysj.org/biophysj/supplemental/S0006-3495(09)00570-0.

We are grateful to Dr. N. Szentandrassy for performing part of the experiments, to Dr. R. Ambrosini for assistance in statistical analysis, to F. Canella for her help with the simulations, and to Dr. E. Grandi for her critical review of the manuscript.

This work was partially funded by an institutional grant to A.Z. (Fondo di Ateneo per la Ricerca, Università Milano-Bicocca 2007) and by Hospal SpA grant to S.S.

REFERENCES

1. Sanguinetti, M. C., N. K. Jurkiewicz, A. Scott, and P. K. Siegl. 1991. Isoproterenol antagonizes prolongation of refractory period by the class III antiarrhythmic agent E-4031 in guinea pig myocytes. Mechanism of action. *Circ. Res.* 68:77–84.
2. Marx, S. O., J. Kurokawa, S. Reiken, H. Motoike, J. D'Armiento, et al. 2002. Requirement of a macromolecular signaling complex for β adrenergic receptor modulation of the KCNQ1-KCNE1 potassium channel. *Science.* 295:496–499.
3. Volders, P. G. A., M. Stengl, J. M. van Opstal, U. Gerlach, R. L. H. M. Spatjens, et al. 2003. Probing the contribution of I_{Ks} to canine ventricular repolarization: key role for β-adrenergic receptor stimulation. *Circulation.* 107:2753–2760.
4. Chen, H., L. A. Kim, S. Rajan, S. Xu, and S. A. N. Goldstein. 2003. Charybdotoxin binding in the I_{Ks} pore demonstrates two MinK subunits in each channel complex. *Neuron.* 40:15–23.
5. Morin, T. J., and W. R. Kobertz. 2008. Counting membrane-embedded KCNE $\pm$ subunits in functioning K^+ channel complexes. *Proc. Natl. Acad. Sci. USA.* 105:1478–1482.
6. Wang, Q., M. E. Curran, I. Splawski, T. C. Burn, J. M. Millholland, et al. 1996. Positional cloning of a novel potassium channel gene: KVLQT1 mutations cause cardiac arrhythmias. *Nat. Genet.* 12:17–23.

7. Schwartz, P. J., S. G. Priori, C. Spazzolini, A. J. Moss, G. M. Vincent, et al. 2001. Genotype-phenotype correlation in the long-QT syndrome: gene-specific triggers for life-threatening arrhythmias. *Circulation.* 103:89–95.
8. Rocchetti, M., V. Freli, V. Perego, C. Altomare, G. Mostacciuolo, et al. 2006. Rate dependency of β-adrenergic modulation of repolarizing currents in the guinea-pig ventricle. *J. Physiol.* 574:183–193.
9. Rocchetti, M., A. Besana, G. B. Gurrola, L. D. Possani, and A. Zaza. 2001. Rate dependency of delayed rectifier currents during the guinea-pig ventricular action potential. *J. Physiol.* 534:721–732.
10. Silva, J., and Y. Rudy. 2005. Subunit interaction determines I_{Ks} participation in cardiac repolarization and repolarization reserve. *Circulation.* 112:1384–1391.
11. Tzounopoulos, T., J. Maylie, and J. P. Adelman. 1998. Gating of I(sK) channels expressed in *Xenopus* oocytes. *Biophys. J.* 74:2299–2305.
12. Imredy, J. P., J. R. Penniman, S. J. Dech, W. D. Irving, and J. J. Salata. 2008. Modeling of the adrenergic response of the human I_{Ks} current (hKCNQ1/hKCNE1) stably expressed in HEK-293 cells. *Am. J. Physiol. Heart Circ. Physiol.* 295:H1867–H1881.
13. Terrenoire, C., C. E. Clancy, J. W. Cormier, K. J. Sampson, and R. S. Kass. 2005. Autonomic control of cardiac action potentials: role of potassium channel kinetics in response to sympathetic stimulation. *Circ. Res.* 96:e25–e34.
14. Brette, F., J. Leroy, J. Y. Le Guennec, and L. Salle. 2006. Ca^{2+} currents in cardiac myocytes: old story, new insights. *Prog. Biophys. Mol. Biol.* 91:1–82.
15. Faber, G. M., and Y. Rudy. 2000. Action potential and contractility changes in [Na(+)](i) overloaded cardiac myocytes: a simulation study. *Biophys. J.* 78:2392–2404.
16. Aizawa, Y., K. Ueda, F. Scornik, J. M. Cordeiro, Y. Wu, et al. 2007. A novel mutation in KCNQ1 associated with a potent dominant negative effect as the basis for the LQT1 form of the long QT syndrome. *J. Cardiovasc. Electrophysiol.* 18:972–977.
17. Walsh, K. B., and R. S. Kass. 1991. Distinct voltage-dependent regulation of a heart-delayed I_K by protein kinases A and C. *Am. J. Physiol. Cell Physiol.* 261:C1081–C1090.
18. Bosch, R. F., R. Gaspo, A. E. Busch, H. J. Lang, G. R. Li, et al. 1998. Effects of the chromanol 293B, a selective blocker of the slow component of the delayed rectifier K^+ current, on repolarization in human and guinea pig ventricular myocytes. *Cardiovasc. Res.* 38:441–450.
19. Dilly, K. W., J. Kurokawa, C. Terrenoire, S. Reiken, W. J. Lederer, et al. 2004. Overexpression of β_2-adrenergic receptors cAMP-dependent protein kinase phosphorylates and modulates slow delayed rectifier potassium channels expressed in murine heart: evidence for receptor/channel co-localization. *J. Biol. Chem.* 279:40778–40787.
20. Chouabe, C., M. D. Drici, G. Romey, J. Barhanin, and M. Lazdunski. 1998. HERG and KvLQT1/IsK, the cardiac K^+ channels involved in long QT syndromes, are targets for calcium channel blockers. *Mol. Pharmacol.* 54:695–703.
21. Lu, Z., K. Kamiya, T. Opthof, K. Yasui, and I. Kodama. 2001. Density and kinetics of I_{Kr} and I_{Ks} in guinea pig and rabbit ventricular myocytes explain different efficacy of I_{Ks} blockade at high heart rate in guinea pig and rabbit: implications for arrhythmogenesis in humans. *Circulation.* 104:951–956.
22. Saucerman, J. J., S. N. Healy, M. E. Belik, J. L. Puglisi, and A. D. McCulloch. 2004. Proarrhythmic consequences of a KCNQ1 AKAP-binding domain mutation: computational models of whole cells and heterogeneous tissue. *Circ. Res.* 95:1216–1224.
23. Silverman, W. R., B. T. Roux, and D. M. Papazian. 2003. Structural basis of two-stage voltage-dependent activation in K^+ hchannels. *Proceedings of the National Academy of Sciences of the United States of America.* 100:2935–2940.
24. Moreno, A. P., J. C. Saez, G. I. Fishman, and D. C. Spray. 1994. Human connexin43 gap junction channels. Regulation of unitary conductances by phosphorylation. *Circ. Res.* 74:1050–1057.
25. Derkach, V., A. Barria, and T. R. Soderling. 1999. Ca^{2+}/calmodulin-kinase II enhances channel conductance of alpha-amino-3-hydroxy-5-methyl-4-isoxazolepropionate type glutamate receptors. *Proc. Natl. Acad. Sci. USA.* 96:3269–3274.
26. Carter, S., J. Colyer, and R. Sitsapesan. 2006. Maximum phosphorylation of the cardiac ryanodine receptor at serine-2809 by protein kinase A produces unique modifications to channel gating and conductance not observed at lower levels of phosphorylation. *Circ. Res.* 98:1506–1513.
27. Seebohm, G., N. Strutz-Seebohm, R. Birkin, G. Dell, C. Bucci, et al. 2007. Regulation of endocytic recycling of KCNQ1/KCNE1 potassium channels. *Circ. Res.* 100:686–692.
28. Varro, A., B. Balati, N. Iost, J. Takacs, L. Virag, et al. 2000. The role of the delayed rectifier component I_{Ks} in dog ventricular muscle and Purkinje fibre repolarization. *J. Physiol.* 523:67–81.
29. Iost, N., L. Virag, M. Opincariu, J. Szecsi, A. Varro, et al. 1998. Delayed rectifier potassium current in undiseased human ventricular myocytes. *Cardiovasc. Res.* 40:508–515.